
TREELearn: A COMPREHENSIVE DEEP LEARNING METHOD FOR SEGMENTING INDIVIDUAL TREES FROM FOREST POINT CLOUDS

Jonathan Henrich*

Chairs of Statistics and Econometrics
Faculty of Economics
University of Göttingen, Germany

Jan van Delden*

Institute of Computer Science
Campus Institute Data Science
University of Göttingen, Germany

Dominik Seidel

Department Spatial Structures and Digitization of Forests
Faculty of Forest Science
University of Göttingen, Germany

Thomas Kneib

Chairs of Statistics and Econometrics
Faculty of Economics
University of Göttingen, Germany

Alexander Ecker

Institute of Computer Science and Campus Institute Data Science, University of Göttingen
Max Planck Institute for Dynamics and Self-Organization
Göttingen, Germany

ABSTRACT

Laser-scanned point clouds of forests make it possible to extract valuable information for forest management. To consider single trees, a forest point cloud needs to be segmented into individual tree point clouds. Existing segmentation methods are usually based on hand-crafted algorithms, such as identifying trunks and growing trees from them, and face difficulties in dense forests with overlapping tree crowns. In this study, we propose TreeLearn, a deep learning-based approach for semantic and instance segmentation of forest point clouds. Unlike previous methods, TreeLearn is trained on already segmented point clouds in a data-driven manner, making it less reliant on pre-defined features and algorithms. Additionally, we introduce a new manually segmented benchmark forest dataset containing 156 full trees, and 79 partial trees, that have been cleanly segmented by hand. This enables the evaluation of instance segmentation performance going beyond just evaluating the detection of individual trees. We trained TreeLearn on forest point clouds of 6665 trees, labeled using the Lidar360 software. An evaluation on the benchmark dataset shows that TreeLearn performs equally well or better than the algorithm used to generate its training data. Furthermore, the method's performance can be vastly improved by fine-tuning on the cleanly labeled benchmark dataset. The TreeLearn code is available from <https://github.com/ecker-lab/TreeLearn>. The data as well as trained models can be found at <https://doi.org/10.25625/VPMPID>.

Keywords Tree Segmentation · Tree Extraction · Tree Isolation · LiDAR · MLS · TLS

*The first two authors contributed equally to this work.

Correspondence: {jonathan.henrich, jan.vandelden}@uni-goettingen.de

1 Introduction

Today, forests are not only exposed to an ever-growing pressure from human use but also to a rapidly changing environment due to climate change. To monitor and understand changes in forest composition and structure as a response to these stressors, as well as for successful forest management, scientists and forest managers require precise and detailed information on the current status of our forests. With recent technological advances, it is possible to collect information on forest structure and composition in an increasingly automated way. For a rapid, detailed and objective assessment of the structural characteristics of forests or individual trees, laser scanning techniques are the most prominent [1, 2, 3]. They allow to create high-resolution (up to mm scale), three-dimensional point clouds of the surfaces in a forest. To analyze such data, it is often useful to separate the point cloud into the individual trees (Figure 1a), e.g. to classify them by their species [4, 5, 6] or to estimate the above-ground biomass [7, 8]. Separating a point cloud into individual trees is an instance segmentation problem: Tree points must first be identified in the point cloud and then each point must be assigned to an individual tree instance. Since manually segmenting forest point clouds is very time-consuming and subjective, there is a need for methods that automate this process.

In this study, we deal with the segmentation of full forest point clouds, as opposed to top-view forest point clouds obtained via airborne laser scanning. Full forest point clouds can be obtained via terrestrial laser scanning, mobile laser scanning or unmanned aerial vehicle laser scanning. The automatic segmentation of such point clouds into individual tree instances is a relatively young research field that has so far been mostly tackled by algorithms based on hand-crafted features. These algorithms usually first identify tree trunks and then assign the remaining points to these trunks based on a fixed set of rules. In early works, these rules were relatively simple. For example, some authors divided the point cloud into clusters and merged them based on distance and relative orientation [9, 10]. Follow-up work building upon these methods included more elaborate local geometry and shape features [11]. More recently, Fu et al. [12] avoided complicated feature computations and proposed to cluster trees from bottom to top in a layer-by-layer manner. Another strand of literature conceptualized the forest as a graph and segmented trees via graph cut [13, 14, 15] or graph pathing methods [16]. Furthermore, some works aimed to incorporate biological theories. For example, Liu et al. [17] constructed features based on plant morphology theory which were then used in a region-growing approach. Similarly, Tao et al. [18] developed a shortest-path algorithm based on metabolic theory, which states that plants tend to minimize the transferring distance to the root. Wang [19] also employed metabolic theory by constructing a superpoint graph where the node features depend on shortest path analysis.

Although modern frameworks achieved significant improvements in performance, automated tree instance segmentation remains prone to errors and usually requires manual post-processing [20], especially in dense forests with heavily intersecting tree crowns. In such scenarios, hand-crafted features and pre-defined heuristics appear to be too inflexible to account for the plethora of possible interactions between trees. Machine learning approaches could overcome these limitations, since features and association rules are derived directly from the data through gradient-based learning. In fact, recent advances in point cloud processing have been dominated by machine learning methods, as indicated by their performance on various point cloud processing benchmarks [e.g., 21, 22, 23]. Although machine learning methods have already been applied to tree segmentation from point clouds [24, 25, 26, 27], they rely on projections into 2D. As a result, they lose information, because the network does not operate on the original point cloud. In contrast, state-of-the-art instance segmentation methods for 3D point clouds operate directly on the three-dimensional input data [28, 29, 30, 31, 32, 33], making them promising candidates for improving existing tree segmentation methods. In this paper, we adapt one of these methods [29] and propose TreeLearn, a comprehensive deep learning method to segment trees from TLS or MLS point clouds. Our method first separates understory and tree points, then projects tree points towards the x- and y-coordinates of the tree base and groups them via density-based clustering.

Regarding the evaluation of the segmentation results, previous research mainly focuses on evaluating the detection of individual trees instead of evaluating the quality of the segmentation itself. There are only a few studies that tackled evaluating the tree-level segmentations [14, 19, 34, 15, 35], most of which have not made their datasets public [14, 16, 15, 35]. Some studies provide publicly available segmentation labels that have been manually corrected. However, they often have shortcomings, such as considering only a small number of trees [36], poor laser scanning coverage [37], or missing understory points [38, 39]. A recent paper addresses these shortcomings by providing a dataset that, among other annotations, includes high-quality segmentation into understory and trees [40]. Such data is crucial for the training and evaluation of machine learning algorithms for the segmentation of forest point clouds. To further increase the diversity of available datasets, we provide a benchmark dataset of a continuous forest with high-quality crown segmentations and classification of points into understory and trees. It contains 156 trees that are completely and 79 trees that are partly within the labeled forest area (Figure 1b). In summary, the main contributions of this study are:

- TreeLearn, a deep-learning-based pipeline that takes forest point clouds as input and outputs both understory points and individual trees.



Figure 1: (a): Predictions generated by TreeLearn on the benchmark forest dataset. (b): A top-view of the manually segmented benchmark forest dataset. For the green area at the edge there are no segmentation labels. It is still included in the dataset since it provides relevant context information for the labeled segment.

- A high-quality hand-segmented forest dataset that can be used to evaluate tree-level segmentation performance.

2 Material and Methods

In the following, we describe both the dataset and our TreeLearn approach in detail. Readers unfamiliar with the technical background can skip directly to the results section.

2.1 Dataset

2.1.1 Scanning Areas

The data basis for model training and validation consists of MLS point clouds from 19 forest plots located in Germany. Eight plots are located near the city of Göttingen, in Lower Saxony, two near Allstedt in Saxony-Anhalt, two near Oppershofen in Hesse, and seven near Lübeck in Schleswig-Holstein. The stands are all dominated by European beech (*Fagus sylvatica* L.) and between 92 and 162 years of age. A detailed description can be found in Neudam et al. [41]. The size of the study plots ranged from 0.9 to 2.2 ha.

2.1.2 Data Acquisition

The plots were recorded in February 2021, in leaf-less condition, using a ZEB Horizon mobile laser scanner (Geoslam Ltd., Nottingham, UK). The device uses a laser to measure the distance and direction to surrounding objects while being carried through a scene. Based on the principle of simultaneous localization and mapping (SLAM) the ZEB Horizon creates a 3D point cloud of the scenery up to a distance of 100 m from the walking trajectory of the operator. Each hand-held walkthrough with the scanner resulted in a file that was used to create a point cloud by conducting the spatial coregistration (actual SLAM) in GeoSlam HUB Version 6 [42]. The resulting point clouds were subsampled to 1 cm resolution to reduce scan artifacts. Additionally, noise filtering was conducted to remove points that are not of interest, such as scanned particles in the air.

2.1.3 Segmentation Labels

To train the neural network in a data-driven manner, we require already segmented forest point clouds. We employ two methods to generate segmentations of the forest point clouds into individual trees and understory: (1) Automatic segmentation for neural network training and (2) manually refined segmentation for fine-tuning and evaluation.

Automatic segmentation To automatically segment the 19 forest point clouds into understory and individual trees, we use the TLS-package from Lidar360 [43] as described by Neudam et al. [41]. The hyperparameters of the Lidar360 software were optimized to produce visually appealing tree segmentations. A minimum size of 10 m was chosen as a requirement for tree classification. Consequently, vegetation that is smaller than 10 m or points belonging to the forest floor were classified as understory. Lidar360’s segmentation algorithm operates on a point cloud that is terrain-normalized, i. e. has a flat ground surface. This is achieved in a separate preprocessing step. To bypass the need for

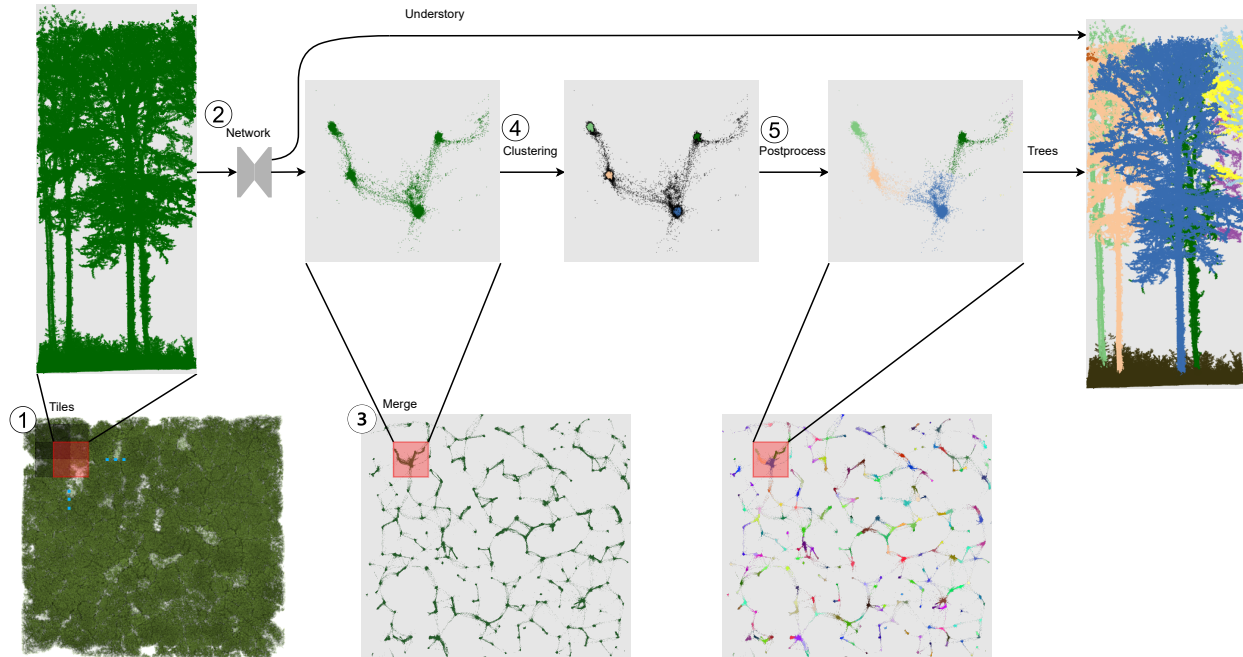


Figure 2: The pipeline for segmenting a forest point cloud. The circled numbers correspond to the steps of the pipeline described in Section 2.2.

terrain normalization for our method, labels from the terrain-normalized data were transferred to the original data. The automatic segmentation contains numerous errors, including multiple trees detected as a single tree, understory identified as part of trees, and inaccuracies in discerning tree boundaries in crowns and branches that are close to each other.

Manually refined segmentation For one forest plot, we manually corrected the segmentation labels generated by Lidar360 with the help of CloudCompare [44] by comparing each tree to all surrounding trees. In a first step, all trees were assessed and corrected if necessary. In a second step, these segmentations were verified and potentially refined.

This was done by two authors (J. H. and J. v. D.). The corrected segmentation covers an area of 112 m by 103 m. It includes 235 trees, 156 of which are located entirely within the segment and 79 of which are partly within the segment (Figure 1b). We appended 11 m of the unlabeled forest point cloud to the labeled segment (Figure 1b, green area at the edge). This area is included in the dataset since it provides relevant context information for the manually segmented parts. The ratio of understory to tree points in the dataset is approximately 2:3. We make the forest plots employed in this work along with the generated segmentation labels available from <https://doi.org/10.25625/VPMPID>.

2.2 TreeLearn Pipeline

The goal of our TreeLearn pipeline is to turn a raw 3D point cloud into groups of points that represent individual trees or understory (Figure 2). More precisely, given a set of 3D points $P = \{p_i = (x_i, y_i, z_i)\}_{i=1}^N$, our pipeline tackles the tasks of semantic and instance segmentation. The goal of semantic segmentation is to achieve a partition of all points into tree and understory points by assigning each point p_i to one of the two classes. The understory class includes all points belonging to the forest floor and smaller vegetation such as bushes or trees smaller than 10 m. The tree class includes all points belonging to trees larger than 10 m. The goal of the following instance segmentation step is to partition the tree points into K (mutually exclusive) individual tree instances. The number of instances K is not known a-priori and must be determined dynamically depending on the input data.

Our complete TreeLearn pipeline consists of the following five steps (Figure 2):

1. Divide the forest point cloud into smaller overlapping rectangular tiles based on the x- and y-coordinates to handle memory restrictions.

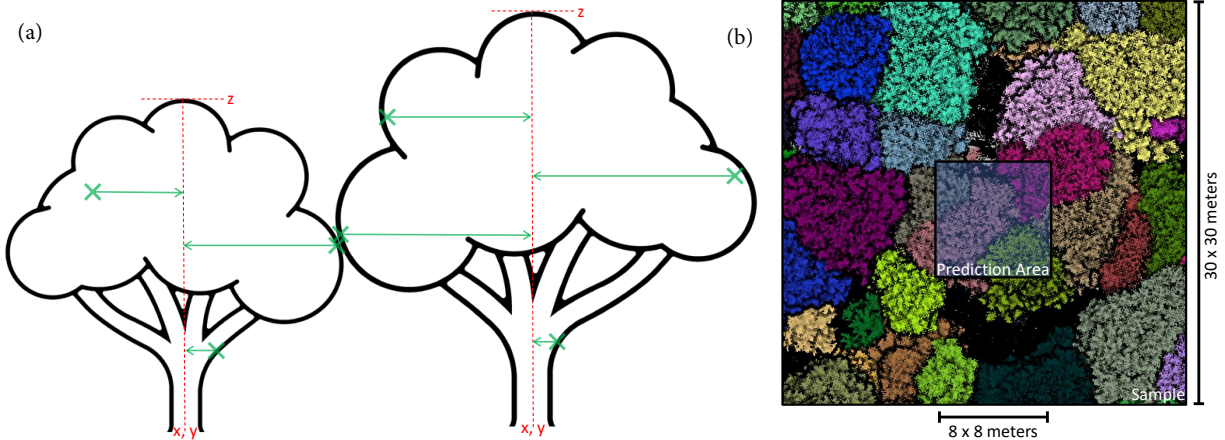


Figure 3: Visualizations regarding offset prediction. (a) depicts offsets for two example trees. The offset is the vector from a point towards the x - and y -coordinates of the tree base and the highest z -coordinate of the tree. For ease of visualization, the offset along the z -dimension is not depicted. (b) visualizes the prediction area in relation to the whole tile. To make sure that the network has the necessary context information, predictions are only produced for the inner blue area of the tile.

2. Use a neural network to predict two quantities for each point in a tile: (1) an offset vector pointing towards the x - and y -coordinates of the tree base and the highest z -coordinate of the tree (Figure 3a), and (2) a semantic score indicating the probability that a point belongs to a tree or understory. This step is carried out separately for each tile generated in step 1.
3. Merge the predictions for the individual tiles to obtain semantic and offset predictions for the whole input point cloud. Project the point coordinates by adding the offset.
4. Apply a clustering algorithm on these projected coordinates to partition the points into individual trees. Disregard points classified as understory.
5. Postprocessing: Assign the remaining points that have not yet been assigned to a tree in step 4 by using a nearest-neighbor criterion.

2.2.1 Step 1: Generate Overlapping Forest Tiles

The point clouds of an entire forest plot in our datasets contain around 20 000 000 points. Processing a point cloud of this size at once using a neural network is infeasible due to memory restrictions. To address this issue, we employ a sliding window approach to process the forest. Predictions are generated for smaller, overlapping tiles that can be processed by the neural network. This approach is inspired by [45] who proposed tiling to process large input images. To create the tiles, we cut out rectangular sections with a fixed edge length of 30 m along the x - and y -axis from the original forest point cloud. The edge length along the z -axis is determined by the highest point. The tiles are generated in an overlapping way with a stride of 4 m.

Prior to generating the tiles, the lidar scans are subsampled with a voxel size of 10cm^3 , leaving only one point within a voxel. The tiles are further filtered using statistical and radius outlier removal [46]. The subsampling and filtering is designed to yield tiles with a reduced number of points, while at the same time preserving the complex structure of trees. Furthermore, the procedure is likely to produce similar results for data obtained by different laser scanners. For example, different laser scanner resolutions above 10 cm do not have an influence on the input data due to the voxelization procedure. This makes our method robust against changes in the input point cloud. Furthermore, results on the original point cloud can be easily obtained by propagating the predictions from the filtered and subsampled point cloud to the original one, e.g. using k -nearest neighbors.

2.2.2 Step 2: Predict Semantic Scores and Offsets

After having generated smaller processable point clouds, we use a neural network to predict two quantities for every point: First, we predict the probability that a point belongs to the semantic classes tree or understory. As these classes are mutually exclusive, this is a binary classification problem. Second, for every point we predict an offset vector [47] that points towards the x - and y -coordinates of the tree base and the highest z -coordinate of the tree. Choosing the

highest z-coordinate of a tree instead of the z-coordinate of the tree base leads to a better separation of trees whose bases are close to each other. Figure 3a visualizes the offset vectors for a few example points.

For semantic and offset prediction, we employ a neural network that takes as input a sparse voxel grid. First, the input space is partitioned into a three-dimensional voxel grid where each voxel is 10 cm^3 in size. Then, for each voxel it is checked whether it contains at least one point. If it does, the voxel is active and will be considered as part of the input to the network. Only active voxels are stored. All other voxels are ignored, hence the name 'sparse voxel grid'.

In this work, a variant of the original U-Net introduced by Ronneberger et al. [45] is used. The network structure of a U-Net can be divided into two main steps. In the contraction step, features are computed in a hierarchical manner by gradually taking into account an increasingly larger context. In the expansion step, these features are propagated to the original points to arrive at rich voxel features that are used for semantic and offset prediction. For a more detailed explanation of the principles, we refer to the original paper [45]. Compared to the original U-Net, the network employed in this work follows the sparse convolution design proposed by Graham et al. [48]. Sparse convolutions differ from regular convolutions in that an activation in the output feature channel occurs only if the voxel at the center of the convolution kernel contains a point. This keeps the number of activations constant, which avoids excessive memory consumption. Furthermore, instead of just stacking convolutions, residual blocks are used to facilitate gradient flow [49]. The residual blocks consist of two 3×3 convolutions and a residual connection. Each contraction step of the U-Net consists of two residual blocks and a 2×2 learned pooling layer implemented by a convolution with stride two. In this work, we employ seven contraction steps. During expansion, it is ensured that the sparse structure is preserved by only propagating activations to voxels that were active during the corresponding contraction step [50]. We adopted the network structure from SoftGroup [28].

To predict the offset and semantic class, two separate heads are used, each of which take as input point features F . These point features $F = \{f_1, \dots, f_N\} \in \mathbb{R}^{N \times D}$ are obtained from the U-Net output by extracting for each of the N original points the corresponding D -dimensional voxel feature. The semantic head maps onto semantic scores and consists of a multilayer perceptron [MLP] with two layers whose parameters are shared between points. Similarly, the offset head uses a shared three-layer MLP and maps onto offset predictions.

Accurate offset prediction is possible only if the corresponding tree base and highest point are within the input tile, so the network can detect them. We therefore predict offsets only for the central $8 \text{ m} \times 8 \text{ m}$ portion of each tile, while the network still receives the whole $30 \text{ m} \times 30 \text{ m}$ tile as input (Figure 3b). This approach ensures that the network has sufficient context information around the points for which it makes predictions. Semantic predictions are also generated only for the inner square.

2.2.3 Step 3: Merge Tiles

After semantic scores and offset vectors have been predicted for all tiles, the points from the inner squares along with their predictions are concatenated to obtain predictions for the full forest point clouds. Predictions made for points outside the inner square are discarded. As the inner squares of neighboring tiles have an overlap of 4 m , multiple predictions for each point are generated. These predictions are then averaged, which reduces artifacts introduced by tiling and leads to smoother transitions between tiles. We calculate the projected coordinates $c_i = p_i + o_i$ by adding the predicted offset (o_i) to the original point (p_i).

2.2.4 Step 4: Identify Tree Instances

Since the goal is to arrive at tree instances, we only consider points with a higher probability to belong to the semantic class tree in this step. If the offset prediction for these points was perfect, the projected coordinates c_i would have exactly the x- and y-coordinate of the corresponding tree base and the z-coordinate of the highest tree point. In practice, the predictions are not perfect, but points belonging to the same tree still group together (Figure 2).

Individual tree clusters are identified by using the coordinates c_i of the full forest point cloud. In a first step, these coordinates are heavily filtered using statistical outlier removal [46]. Specifically, we first calculate for each point the mean distance towards the 100 nearest neighbors. Then all points with an above-average distance are removed, effectively excluding those points located between tree clusters since the point density is lower there. This leads to a better separation between clusters, which mitigates the problem of merged trees. In a second step, the filtered coordinates c_i are used as input to a density-based clustering algorithm [51] following previous works [29, 28]. Specifically, an undirected graph is constructed where an edge between two points exists if their Euclidean distance is smaller than a predefined grouping radius τ_{group} . Clusters are then obtained by identifying all connected components of the graph that consist of at least τ_{min} points. However, it is not guaranteed that all clusters represent complete trees. Some might only consist of small fragments of a tree. To tackle this problem, we employ a small convolutional neural network to classify whether a cluster constitutes a tree or a fragment. The network takes as input the features F of the points

belonging to a cluster and outputs a tree probability. All clusters with a tree probability smaller than 0.5 are discarded. The remaining clusters correspond to the preliminary predicted tree instances.

2.2.5 Step 5: Assign Remaining Points

In the previous step, a large proportion of the points has been assigned to individual tree instances. However, (1) points that were removed by the filtering procedure, (2) points that do not belong to any cluster and (3) points of clusters classified as a fragment remain unassigned (Figure 2, black points in step 4). To assign these points, we opt to use a simple strategy: The k nearest neighbors of these points are determined among points that have already been assigned to trees. These neighbors are calculated based on the projected coordinates c_i instead of the original coordinates. This way, the information provided by the neural network is used. We set $k = 10$, although the exact value is not of great importance.

2.3 Training

The U-Net described in Section 2.2.2 was first trained using the segmentation labels automatically obtained from Lidar360. Since these labels contain numerous mistakes, we refer to them as noisy labels. The model obtained by training on noisy labels was then fine-tuned using the manually corrected labels. We refer to these labels as clean labels. Furthermore, the classifier for the identification of fragments was trained.

2.3.1 Noisy Labels

To generate the training data, we cropped out random areas of size $30 \text{ m} \times 30 \text{ m}$ from the 18 forest plots that have only been automatically segmented. These crops were then subsampled and filtered using the procedure described in Section 2.2.1. In total, 20 000 crops were generated.

To train the network, we calculate loss values on the predictions within the inner area of a crop, as displayed in Figure 3b. This way, the neural network almost always has enough context information. To supervise the offset prediction, we use the average L1-distance across tree points between the actual and predicted offset vector. For the semantic predictions, we use the binary cross entropy loss function and further scale it by a factor of 50 to obtain a similar magnitude to the offset loss. The offset and semantic loss are then summed to obtain the loss used for training. The U-Net was trained for 150 000 iterations using the AdamW optimizer [52] with a weight decay of 10^{-3} and $\beta = [0.9, 0.999]$. The batch size was set to 4. We further chose a cosine learning rate schedule [53] with a warm up period of 6250 iterations and a maximum/minimum learning rate of $3 \times 10^{-3}/5 \times 10^{-6}$. Parameters pre-trained for 3D instance segmentation from [54] were used as initialization for the model.

2.3.2 Clean Labels

Following the same procedure as described in Section 2.3.1, 4500 training crops were generated for the cleanly labeled forest plot. For fine-tuning, the model was initialized with parameters obtained by training with noisy labels. From there, the network was trained for 3125 iterations without warm up and a maximum/minimum learning rate of $4 \times 10^{-5}/5 \times 10^{-7}$. Otherwise, the training specifications were the same as described in Section 2.3. Apart from fine-tuning, training the model from scratch with cleanly labeled data was also attempted, but was not successful due to overfitting.

2.3.3 Classifier

To obtain training samples for the classifier, predicted tree instances with an intersection over union [IoU] > 0.75 with a ground truth tree were given the label ‘tree’ and predicted tree instances with an IoU < 0.25 were given the label ‘fragment’. These samples were generated from predictions on the noisy training data. The binary cross entropy loss was used to supervise the class prediction. The network was trained for 400 iterations using the AdamW optimizer with the same specifications as for the U-Net and a batch size of 16. A cosine learning rate schedule was employed with a maximum/minimum learning rate of $5 \times 10^{-4}/1 \times 10^{-7}$.

2.4 Evaluation Metrics

2.4.1 Semantic Segmentation Evaluation: Tree vs. Understory

For semantic segmentation evaluation, we assess how well the method divides the points into the semantic classes understory and tree. As a metric, we choose the accuracy, which is the number of correctly predicted points divided

by the total number of points. We report evaluation results on the point cloud subsampled with a voxel size of 10cm^3 (see Section 2.2.1). This avoids a disproportionate weighting of regions with higher point densities like the trunks.

2.4.2 Instance Detection Evaluation

For instance detection evaluation, we are interested in how well the predicted tree instances match the ground truth tree instances. Specifically, we consider true positive predictions (TP), false negative predictions (FN) and false positive predictions (FP) as defined in Fu et al. [12]: A tree prediction is TP if, in principle, it has a clear match (defined below) to a ground truth tree. If a tree is predicted to belong to a larger nearby tree or to the understory, it is FN . Finally, if a prediction is no complete tree instance but only a fragment, it is FP . It should be noted that one prediction consisting of two merged trees only results in one FN . The larger tree of the two still counts as detected using the above definition.

To automatically identify TP , FP and FN predictions, we first calculate the pointwise IoU between all predictions and ground truths. Then, Hungarian matching [55] is performed to assign predictions to ground truths. To avoid the assignment of fragments to ground truth trees, we set a minimum IoU of 0.3 as a requirement for a match. Matched predictions, non-matched predictions and non-matched ground truths are considered TP , FP and FN respectively. Trees at the edge of the segmented area are often only partially within the point cloud and might consist of only one branch within the segmented area. If this one branch is falsely assigned to another tree, this results in a FN . This is misleading since the actual tree, which is not within the evaluation area, might be correctly detected. Therefore, we consider only trees that are fully within the prediction area (156 trees) for this part of the evaluation. Likewise, only predictions whose maximum overlap is with one of these 156 trees, are taken into account.

2.4.3 Instance Segmentation Evaluation

For the evaluation of instance segmentation, we assess how well the points of the predicted tree instances match the points of the corresponding ground truth tree instances. Since detection errors represent a different quality of mistakes, we do not consider predicted tree instances that are associated with a detection error. This includes (1) FP predicted tree instances (fragments) and (2) predicted tree instances that consist of more than one ground truth tree (merged predictions). To evaluate the instance segmentation, we use precision, recall and the F1-score:

$$Prec = \frac{TP}{TP + FP} \quad Rec = \frac{TP}{TP + FN} \quad F1 = 2 * \frac{Prec * Rec}{Prec + Rec} \quad (1)$$

Note that TP , FP and FN are here defined at the point-level, not the instance-level. The metrics are calculated separately for every predicted tree instance with the corresponding ground truth tree points as positives and all other points as negatives. Then, they are averaged over all predictions that are taken into account.

Not all locations of a tree are equally difficult to segment correctly. For example, points near the trunk are usually easier to assign than points farther outside where there are many interactions with other trees. To quantify how well different parts of the trees are segmented, we partition the points of a prediction and the corresponding tree into 10 subsets and calculate the metric for each subset. For each subset, the metric is then averaged across predictions. We propose two axes for partitioning: (1) horizontal distance to the trunk, and (2) vertical distance to the forest floor. For the horizontal partition, the i -th subset contains all points with a horizontal distance to the trunk between $\frac{i-1}{10}r$ and $\frac{i}{10}r$ where r is the maximum distance. For the vertical partition, the i -th subset contains all points with a vertical distance to the floor between $\frac{i-1}{10}h$ and $\frac{i}{10}h$ where h is the height of the tree. We set $i = 1, \dots, 10$.

2.5 Model Selection

We have one cleanly labeled forest plot. To report unbiased estimates of model performance, we split it into two parts: one used for model selection (validation set) and the other one for estimating model performance (test set). To make the best use of the available data, we used each part once as the validation set and evaluated the performance on the other, and vice versa. When training with the noisy labels, the parameters with the lowest offset loss on the validation set were selected. The validation set was then also used to fine-tune the selected parameters as described in Section 2.3.2. In this case, the parameters after the last training iteration were selected without any selection criterion. This way, test performance on the full cleanly labeled forest plot can be evaluated for both noisy and clean label training.

Apart from the model parameters, the proposed method has the two hyperparameters τ_{group} and τ_{min} as described in Section 2.2.4. We set $\tau_{\text{min}} = 100$. Since it is virtually impossible that trees consist of less than 100 points, this ensures that no trees are discarded during grouping. The choice of such a low number inevitably results in fragments. However,

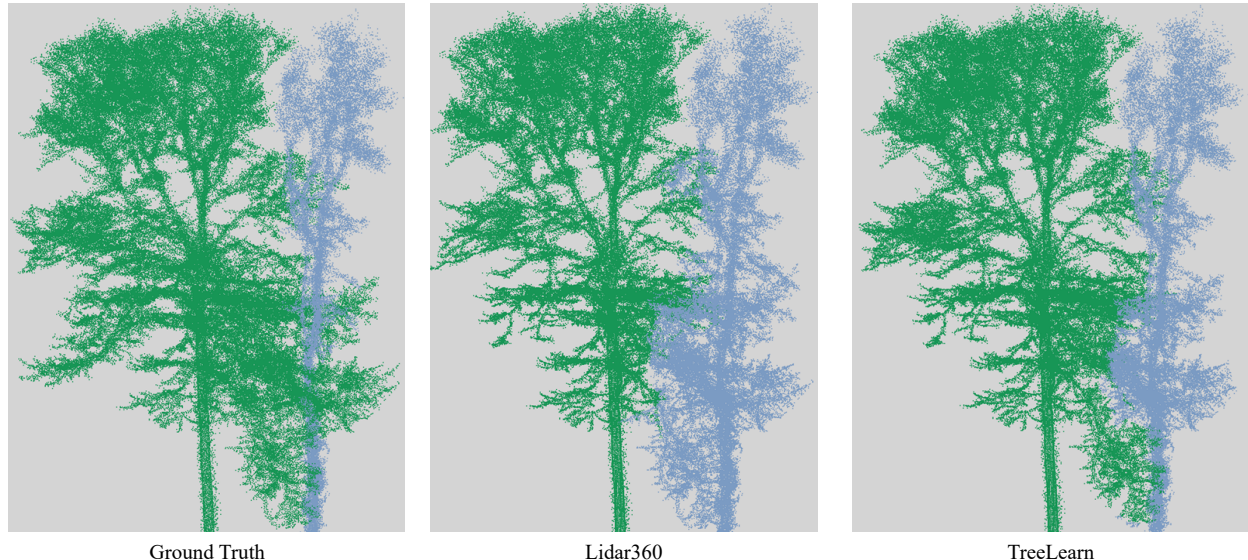


Figure 4: Comparison of instance segmentation results for two heavily intertwined trees. The result of TreeLearn has some errors, but is better than Lidar360.

	Semantic Segmentation	Detection		Instance Segmentation
	Accuracy	<i>FP</i> Predictions	<i>FN</i> Trees	<i>F1</i>
Lidar360	99.59	1	1	93.21
Noisy Labels Training	99.64	0	0	94.07
Clean Labels Fine-tuning	99.86	0	1	98.21

Table 1: Overall results. Instance segmentation results averaged across predictions. Semantic and instance segmentation results in %.

we found that the classifier successfully identifies such fragments. We further set $\tau_{\text{group}} = 0.2$ m. The exact value is not of great importance since the method is robust to changes in the grouping radius. An experiment that indicates the robustness of our method to different τ_{group} as well as the effectiveness of the classifier and the filtering procedure described in Section 2.2.4 can be found in A.

3 Results

TreeLearn performs three tasks: segmenting points into understory and trees, detecting individual trees and assigning points to their corresponding tree instance. In the following, we evaluate the system’s performance on each of these tasks using our manually labeled benchmark dataset.

We trained TreeLearn supervised on labels generated automatically by an existing software (‘Lidar360’, [43]). The segmentation results of this software have mistakes, hence the need to improve. Our first, perhaps surprising, finding is that the segmentation algorithm learned from these ‘noisy’ labels performs better than the algorithm that generated the training data, i. e. a machine learning approach can extract more consistent segmentation rules than its ‘teacher’. On average, TreeLearn improves instance segmentation performance measured by the F1-score from 93.21 % (Lidar360) to 94.07 % (Table 1).

Fine-tuning TreeLearn on the clean manually labeled forest plot improves the result drastically to an instance segmentation performance of 98.21 % (for an example, see Figure 4). Both variations of TreeLearn also produce a better separation of trees and understory. In particular, the semantic segmentation accuracy increases from 99.59 % (Lidar360) to 99.86 % for the fine-tuned TreeLearn. An improved performance compared to Lidar360 can also be observed for the detection results. Lidar360 fails to detect one tree (*FN*) and produces one prediction that does not actually constitute a tree (*FP*). In contrast, TreeLearn produces one *FN* in the fine-tuned setting, while producing no

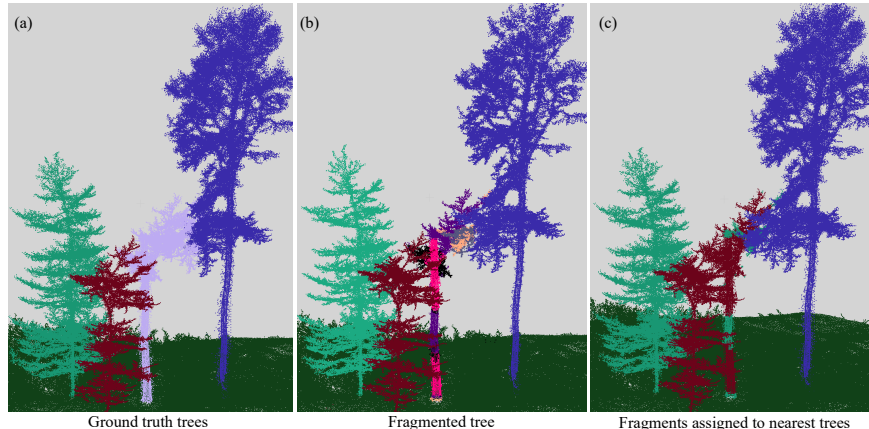


Figure 5: Tree not detected. (a) shows the ground truth trees. (b) shows the prediction before applying the classifier. The tree that is not detected is fragmented into smaller parts. (c) shows the final prediction. The fragments are identified and assigned to nearby tree instances.

	Precision	Recall	$F1$
Lidar360	92.52	94.81	93.21
Noisy Labels Training	93.58	95.4	94.07
Clean Labels Fine-tuning	97.94	98.62	98.21

Table 2: Instance segmentation results averaged across predictions. All values in %.

detection errors without fine-tuning. However, detection errors are generally rare, so there is no conclusive evidence that one method performs better than the other in this regard.

The ground truth tree that was not detected by our method is depicted in Figure 5a. It can be seen that the points belonging to this tree have been assigned to two nearby trees (Figure 5c). To understand why this happened, it is instructive to look at the prediction before applying the classifier for the identification of fragments. At this stage, the tree is also not correctly detected but rather consists of multiple small fragments (Figure 5b). The result depicted in Figure 5c emerges since the classifier identifies these fragments and assigns them to nearby trees as described in Section 2.2.4. The fragments are a consequence of the filtered projected coordinates (see Section 2.2.4) not being sufficiently concentrated at a single point for the density-based clustering algorithm to detect them as a single cluster. Manually, it would be easy to fix the failed detection, as the projected points of the tree are clearly separated from other trees.

3.1 Instance Segmentation

In this section, we take a more detailed look at the instance segmentation results. In addition to an overall better F1-score, both TreeLearn settings achieve a better precision and recall value (Table 2). We also observe that, irrespective of the method, recall is higher than precision. We conjecture that this is the case because the branches of larger trees often protrude into smaller trees. If these branches are then incorrectly assigned to the smaller tree, the precision of the smaller tree is affected considerably. On the other hand, a falsely assigned branch does not affect the recall of the larger tree to the same degree.

A more fine-grained understanding can be achieved by evaluating the segmentation performance at different locations of a tree. For this, we partition the points of a prediction and the corresponding tree into subsets based on horizontal distance to the tree trunk and vertical distance to the forest floor as described in Section 2.4.3. Figure 6 shows precision, recall and F1-scores for the two partitions. For both methods, performance decreases for points farther away from the trunk due to increased interactions with other trees. However, this trend is less pronounced for TreeLearn, indicating a certain stability with respect to the distance to the trunk. This is especially true for the fine-tuned model.

For the vertical partition of the trees, there is a visible performance low for intermediate heights, where trees tend to have their maximum width. Furthermore, the area directly above the ground poses difficulties. This is most likely due to understory and tree points that are hard to distinguish from each other (see e.g. Figure 7).

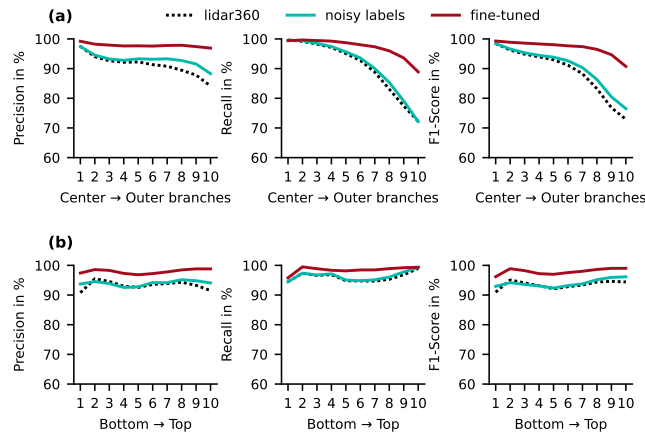


Figure 6: Instance segmentation performance. (a) shows metrics for segments along the x- and y- axis. (b) shows metrics for segments along the z-axis.

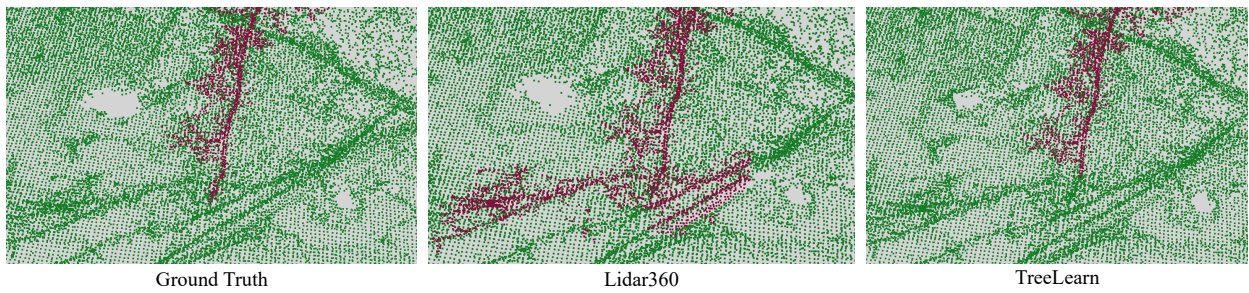


Figure 7: Comparison of semantic segmentation results. Lidar360 assigns completely unrelated points. TreeLearn is more conservative.

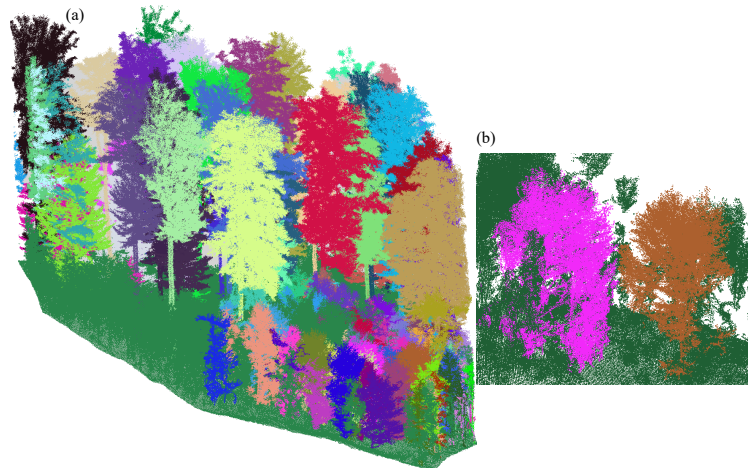


Figure 8: Segmentation result on out-of-domain forest plot. TreeLearn is able to correctly segment the large trees (a). The smaller trees, that form a densely grown understory, are partly detected, but contain errors (b).

3.2 Qualitative Test Results

We have one additional forest plot that was used neither for training nor for validation. Regarding tree species composition and size, the plot is similar to the ones used during training. However, it has a denser understory than the benchmark forest plot and also a steeper incline that has not been present in the training data (more than 35 %). We apply our method on this forest plot to see how well it deals with this novel scenario. Since no manually corrected segmentation labels are available, no quantitative evaluation is possible. TreeLearn is able to correctly identify a large proportion of the trees, despite this incline. Even many of the small trees are correctly identified by our method (Figure 8).

4 Discussion

In this study, we introduced a comprehensive method for segmenting individual trees from high-resolution forest point clouds, requiring no preprocessing in the form of understory removal or terrain normalization. To the best of our knowledge, this work is the first to tackle this task with a deep learning method that operates directly on point cloud data. TreeLearn is based on a 3D U-Net for pointwise feature prediction, followed by clustering and postprocessing to derive instance predictions. As demonstrated in Section 3, our method performs equally well or better than Lidar360 in all aspects, despite being trained on data segmented by it. Furthermore, the results indicate that major performance increases can be achieved by fine-tuning the network on small amounts of high-quality labeled data. In addition to the segmentation method, we introduced a new benchmark dataset, that allows for the evaluation of instance segmentation results. This is an important step towards a better comparability of different tree segmentation methods.

One limitation of TreeLearn is that the training data determines the properties of the model. For example, in our data trees with a height of less than 10 meters were labeled as understory. If smaller trees should be recognized, the training data must be adapted accordingly. Furthermore, only beech forests have been used during training. We expect a drop in performance when segmenting point clouds of forests with a highly different structure. Incorporating more diverse data during training or fine-tuning can alleviate this issue. On a positive note, this also means that the model will benefit from any tree segmentation dataset contributions made by the community.

Another way to improve TreeLearn is to develop a more sophisticated tree identification algorithm. In our work, we used simple density-based clustering on the filtered projected coordinates (see Section 2.2.4). As shown in Figure 5, this can lead to multiple clusters being predicted for a single tree, even though these clusters are in principle clearly separated from other trees. For example, a hierarchical clustering algorithm similar to the one proposed by Chen et al. [54] might lead to a better result. Another way to enhance the capabilities of our framework is to train with more refined semantic classes. For example, it is possible to subdivide tree points into woody parts and leaves. If the corresponding training data is available, this can be easily integrated into the framework. Further potential of TreeLearn lies in the usage of the tree-level U-Net features for other tasks of interest. In our work, we already used the features of tree clusters to classify whether they are valid trees or fragments. Other tasks of interest are, for example, tree species classification, biomass prediction or tree health assessment. This way, our model could serve as a starting point to build a more general forest inventory framework. However, it should be noted that currently it is not straightforward to train tree-level tasks in an end-to-end manner because of the in-between clustering step that is necessary to obtain trees.

In conclusion, we have presented a powerful and adaptable deep-learning-based method for tree instance segmentation of forest point clouds, as well as a benchmark dataset for evaluating instance segmentation performance. Given the positive results of our study, we hope to encourage fellow researchers to further explore the potential of point-cloud-based deep learning methods in the analysis of forests. Going forward, our method could be used as a building block in a more general forest inventory framework. Single-tree point clouds, as provided by our fully automatic approach, are valuable information for forest scientists and forest managers, as they can be used to derive single-tree parameters. Such data is urgently needed to plan silviculture activities, to estimate carbon stocks or harvest yields, and for many others tasks.

Declaration of Competing Interest

The authors declare that they have no known competing financial interests or personal relationships that could have appeared to influence the work reported in this paper.

References

- [1] X. Liang, J. Hyypä, A. Kukko, H. Kaartinen, A. Jaakkola, X. Yu, The use of a mobile laser scanning system for mapping large forest plots, *IEEE Geoscience and Remote Sensing Letters* 11 (2014) 1504–1508.
- [2] M. Disney, Terrestrial lidar: a three-dimensional revolution in how we look at trees, *New Phytologist* 222 (2019) 1736–1741.
- [3] K. Calders, J. Adams, J. Armston, H. Bartholomeus, S. Bauwens, L. P. Bentley, J. Chave, F. M. Danson, M. Demol, M. Disney, et al., Terrestrial laser scanning in forest ecology: Expanding the horizon, *Remote Sensing of Environment* 251 (2020) 112102.
- [4] L. Terry, K. Calders, M. Disney, N. Origo, Y. Malhi, G. Newnham, P. Raunonen, H. Verbeeck, et al., Tree species classification using structural features derived from terrestrial laser scanning, *ISPRS Journal of Photogrammetry and Remote Sensing* 168 (2020) 170–181.
- [5] Z. Xi, C. Hopkinson, S. B. Rood, D. R. Peddle, See the forest and the trees: Effective machine and deep learning algorithms for wood filtering and tree species classification from terrestrial laser scanning, *ISPRS Journal of Photogrammetry and Remote Sensing* 168 (2020) 1–16.
- [6] D. Seidel, P. Annighöfer, A. Thielman, Q. E. Seifert, J.-H. Thauer, J. Glatthorn, M. Ehbrecht, T. Kneib, C. Ammer, Predicting tree species from 3d laser scanning point clouds using deep learning, *Frontiers in Plant Science* 12 (2021) 635440.
- [7] D. Xu, H. Wang, W. Xu, Z. Luan, X. Xu, Lidar applications to estimate forest biomass at individual tree scale: Opportunities, challenges and future perspectives, *Forests* 12 (2021) 550.
- [8] B. Brede, L. Terry, N. Barbier, H. M. Bartholomeus, R. Bartolo, K. Calders, G. Derroire, S. M. K. Moorthy, A. Lau, S. R. Levick, et al., Non-destructive estimation of individual tree biomass: Allometric models, terrestrial and uav laser scanning, *Remote Sensing of Environment* 280 (2022) 113180.
- [9] J. Trochta, M. Krček, T. Vrška, K. Král, 3D Forest: An application for descriptions of three-dimensional forest structures using terrestrial LiDAR, *PloS one* 12 (2017) e0176871.
- [10] P. Raunonen, E. Casella, K. Calders, S. Murphy, M. Åkerblom, M. Kaasalainen, Massive-scale tree modelling from TLS data, *ISPRS Ann. Photogramm. Remote Sens. Spat. Inf. Sci* 2 (2015) 189.
- [11] A. Burt, M. Disney, K. Calders, Extracting individual trees from lidar point clouds using treeseg, *Methods in Ecology and Evolution* 10 (2019) 438–445.
- [12] H. Fu, H. Li, Y. Dong, F. Xu, F. Chen, Segmenting individual tree from tls point clouds using improved dbscan, *Forests* 13 (2022) 566.
- [13] L. Zhong, L. Cheng, H. Xu, Y. Wu, Y. Chen, M. Li, Segmentation of individual trees from tls and mls data, *IEEE Journal of Selected Topics in Applied Earth Observations and Remote Sensing* 10 (2016) 774–787.
- [14] J. Heinzl, M. O. Huber, Constrained spectral clustering of individual trees in dense forest using terrestrial laser scanning data, *Remote Sensing* 10 (2018) 1056.
- [15] Z. Xi, C. Hopkinson, 3d graph-based individual-tree isolation (treeiso) from terrestrial laser scanning point clouds, *Remote Sensing* 14 (2022) 6116.
- [16] D. Wang, X. Liang, G. I. Mofack, O. Martin-Ducup, Individual tree extraction from terrestrial laser scanning data via graph pathing, *Forest Ecosystems* 8 (2021) 1–11.
- [17] Q. Liu, W. Ma, J. Zhang, Y. Liu, D. Xu, J. Wang, Point-cloud segmentation of individual trees in complex natural forest scenes based on a trunk-growth method, *Journal of Forestry Research* 32 (2021) 2403–2414.
- [18] S. Tao, F. Wu, Q. Guo, Y. Wang, W. Li, B. Xue, X. Hu, P. Li, D. Tian, C. Li, et al., Segmenting tree crowns from terrestrial and mobile lidar data by exploring ecological theories, *ISPRS Journal of Photogrammetry and Remote Sensing* 110 (2015) 66–76.
- [19] D. Wang, Unsupervised semantic and instance segmentation of forest point clouds, *ISPRS Journal of Photogrammetry and Remote Sensing* 165 (2020) 86–97.
- [20] O. Martin-Ducup, G. Mofack, D. Wang, P. Raunonen, P. Ploton, B. Sonké, N. Barbier, P. Coutron, R. Pélissier, Evaluation of automated pipelines for tree and plot metric estimation from TLS data in tropical forest areas, *Annals of botany* 128 (2021) 753–766.
- [21] I. Armeni, O. Sener, A. R. Zamir, H. Jiang, I. Brilakis, M. Fischer, S. Savarese, 3d semantic parsing of large-scale indoor spaces, in: 2016 IEEE Conference on Computer Vision and Pattern Recognition (CVPR), IEEE, 2016, pp. 1534–1543.

- [22] A. Dai, A. X. Chang, M. Savva, M. Halber, T. Funkhouser, M. Nießner, Scannet: Richly-annotated 3d reconstructions of indoor scenes, in: 2017 IEEE Conference on Computer Vision and Pattern Recognition (CVPR), IEEE, 2017, pp. 2432–2443.
- [23] T. Hackel, N. Savinov, L. Ladicky, J. D. Wegner, K. Schindler, M. Pollefeys, Semantic3d. net: A new large-scale point cloud classification benchmark, arXiv preprint arXiv:1704.03847 (2017).
- [24] J. Wang, X. Chen, L. Cao, F. An, B. Chen, L. Xue, T. Yun, Individual rubber tree segmentation based on ground-based lidar data and faster r-cnn of deep learning, *Forests* 10 (2019) 793.
- [25] L. Windrim, M. Bryson, Forest tree detection and segmentation using high resolution airborne lidar, in: 2019 IEEE/RSJ International Conference on Intelligent Robots and Systems (IROS), IEEE, 2019, pp. 3898–3904.
- [26] L. Windrim, M. Bryson, Detection, segmentation, and model fitting of individual tree stems from airborne laser scanning of forests using deep learning, *Remote Sensing* 12 (2020) 1469.
- [27] L. Chang, H. Fan, N. Zhu, Z. Dong, A two-stage approach for individual tree segmentation from tls point clouds, *IEEE Journal of Selected Topics in Applied Earth Observations and Remote Sensing* 15 (2022) 8682–8693.
- [28] T. Vu, K. Kim, T. M. Luu, T. Nguyen, C. D. Yoo, Softgroup for 3d instance segmentation on point clouds, in: Proceedings of the IEEE/CVF Conference on Computer Vision and Pattern Recognition, 2022, pp. 2708–2717.
- [29] L. Jiang, H. Zhao, S. Shi, S. Liu, C.-W. Fu, J. Jia, Pointgroup: Dual-set point grouping for 3d instance segmentation, in: Proceedings of the IEEE/CVF conference on computer vision and Pattern recognition, 2020, pp. 4867–4876.
- [30] J. Sun, C. Qing, J. Tan, X. Xu, Superpoint transformer for 3d scene instance segmentation, arXiv preprint arXiv:2211.15766 (2022).
- [31] J. Schult, F. Engelmann, A. Hermans, O. Litany, S. Tang, B. Leibe, Mask3d for 3d semantic instance segmentation, arXiv preprint arXiv:2210.03105 (2022).
- [32] Y. Wu, M. Shi, S. Du, H. Lu, Z. Cao, W. Zhong, 3d instances as 1d kernels, in: Computer Vision–ECCV 2022: 17th European Conference, Tel Aviv, Israel, October 23–27, 2022, Proceedings, Part XXIX, Springer, 2022, pp. 235–252.
- [33] T. D. Ngo, B.-S. Hua, K. Nguyen, Isbnet: a 3d point cloud instance segmentation network with instance-aware sampling and box-aware dynamic convolution, arXiv preprint arXiv:2303.00246 (2023).
- [34] P. Wilkes, M. I. Disney, J. Armston, H. Bartholomeus, L. P. Bentley, B. Brede, A. Burt, K. Calders, C. Chavana-Bryant, D. Clewley, et al., Tls2trees: a scalable tree segmentation pipeline for tls data, *bioRxiv* (2022) 2022–12.
- [35] M. Wielgosz, S. Puliti, P. Wilkes, R. Astrup, Point2tree (p2t)–framework for parameter tuning of semantic and instance segmentation used with mobile laser scanning data in coniferous forest, arXiv preprint arXiv:2305.02651 (2023).
- [36] K. Calders, G. Newnham, A. Burt, S. Murphy, P. Raunonen, M. Herold, D. Culvenor, V. Avitabile, M. Disney, J. Armston, et al., Nondestructive estimates of above-ground biomass using terrestrial laser scanning, *Methods in Ecology and Evolution* 6 (2015) 198–208.
- [37] H. Weiser, J. Schäfer, L. Winiwarter, N. Krašovec, F. E. Fassnacht, B. Höfle, Individual tree point clouds and tree measurements from multi-platform laser scanning in german forests, *Earth System Science Data* 14 (2022) 2989–3012.
- [38] A. Tockner, C. Gollob, T. Ritter, A. Nothdurft, LAUTx - Individual Tree Point Clouds from Austrian forest Inventory plots, <https://zenodo.org/record/6560112>, 2022. Available at Zenodo.
- [39] K. Calders, N. Origo, A. Burt, M. Disney, J. Nightingale, P. Raunonen, M. Åkerblom, Y. Malhi, P. Lewis, Realistic forest stand reconstruction from terrestrial lidar for radiative transfer modelling, *Remote Sensing* 10 (2018) 933.
- [40] S. Puliti, G. Pearse, P. Surovỳ, L. Wallace, M. Hollaus, M. Wielgosz, R. Astrup, For-instance: a uav laser scanning benchmark dataset for semantic and instance segmentation of individual trees, arXiv preprint arXiv:2309.01279 (2023).
- [41] L. C. Neudam, J. M. Fuchs, E. Mjema, A. Johannmeier, C. Ammer, P. Annighöfer, C. Paul, D. Seidel, Simulation of silvicultural treatments based on real 3d forest data from mobile laser scanning point clouds, *Trees, Forests and People* (2023) 100372.
- [42] G. Ltd, Geoslam hub version 6, 2020. URL: <https://geoslam.com>.
- [43] GreenValley International, Lidar360 point cloud post-processing software, 2022. URL: <https://greenvalleyintl.com/LiDAR360>, accessed: 26.10.2022.

- [44] Daniel Girardeau-Montaut, Cloudcompare, 2022. URL: <https://www.cloudcompare.org/>.
- [45] O. Ronneberger, P. Fischer, T. Brox, U-net: Convolutional networks for biomedical image segmentation, in: International Conference on Medical image computing and computer-assisted intervention, Springer, 2015, pp. 234–241.
- [46] Q.-Y. Zhou, J. Park, V. Koltun, Open3D: A modern library for 3D data processing, 2018. doi:10.48550/ARXIV.1801.09847.
- [47] C. R. Qi, O. Litany, K. He, L. J. Guibas, Deep hough voting for 3d object detection in point clouds, in: proceedings of the IEEE/CVF International Conference on Computer Vision, 2019, pp. 9277–9286.
- [48] B. Graham, M. Engelcke, L. Van Der Maaten, 3d semantic segmentation with submanifold sparse convolutional networks, in: Proceedings of the IEEE conference on computer vision and pattern recognition, 2018, pp. 9224–9232.
- [49] K. He, X. Zhang, S. Ren, J. Sun, Deep residual learning for image recognition, in: Proceedings of the IEEE conference on computer vision and pattern recognition, 2016, pp. 770–778.
- [50] S. Contributors, Spconv: Spatially sparse convolution library, <https://github.com/traveller59/spconv>, 2022.
- [51] M. Ester, H.-P. Kriegel, J. Sander, X. Xu, et al., A density-based algorithm for discovering clusters in large spatial databases with noise., in: kdd, volume 96, 1996, pp. 226–231.
- [52] I. Loshchilov, F. Hutter, Decoupled weight decay regularization, 2017. doi:10.48550/ARXIV.1711.05101.
- [53] I. Loshchilov, F. Hutter, Sgdr: Stochastic gradient descent with warm restarts, 2016. doi:10.48550/ARXIV.1608.03983.
- [54] S. Chen, J. Fang, Q. Zhang, W. Liu, X. Wang, Hierarchical aggregation for 3d instance segmentation, in: Proceedings of the IEEE/CVF International Conference on Computer Vision, 2021, pp. 15467–15476.
- [55] H. W. Kuhn, The hungarian method for the assignment problem, Naval research logistics quarterly 2 (1955) 83–97.

A Experiment for filtering, classifier and grouping radius

The filtering procedure prior to clustering is applied on the projected point coordinates and serves the purpose of removing uncertain points between distinct tree clusters. The purpose of this filtering is to mitigate the occurrence of merged trees, which would lead to FN predictions. Clusters are obtained by applying a density-based clustering algorithm on the filtered points. These clusters are then processed with a classification network to identify fragments (FP predictions).

To assess the effectiveness of the filtering procedure and classifier to tackle FN and FP predictions, we ran TreeLearn trained with noisy labels under three different conditions: (1) no filtering and no classification (2) filtering but no classification (3) both filtering and classification. For each condition, we evaluated the method with grouping radii τ_{group} ranging from 0.1 m to 1 m in steps of 0.1 m. Without filtering and classification, there is a non-zero number of FP and FN predictions irrespective of the grouping radius. Adding filtering (condition 2), entirely removes the occurrence of FN predictions, while leaving FP predictions basically unchanged. Only when using both filtering and classification (condition 3), can the number of FN and FP predictions be reduced to zero for all grouping radii except $\tau_{\text{group}} = 1$ m. The results of the experiment are visualized in Figure 9. Two conclusions can be drawn from this experiment: First, the proposed filtering and classification procedure effectively tackles FN and FP predictions. Second, the dependence of our method on hyperparameters is low. It produces the same detection results for a large range of τ_{group} values. Furthermore, setting $\tau_{\text{min}} = 100$ does not impair the method, since it is virtually impossible that trees only consist of such a small number of points.

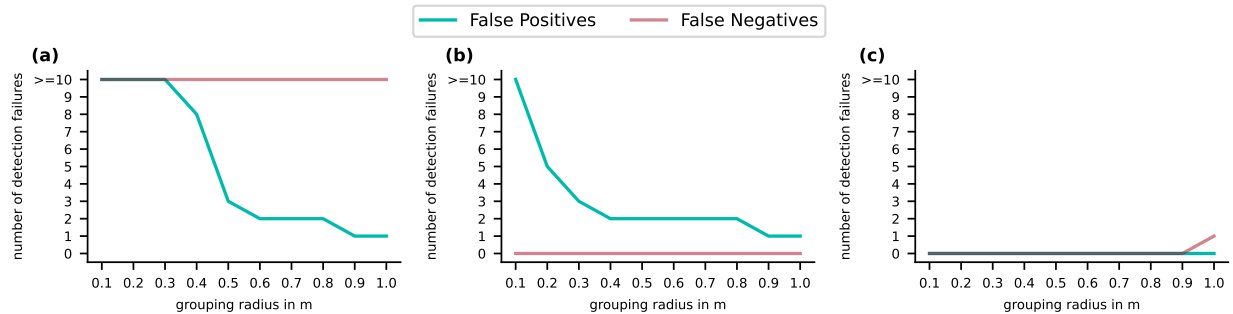


Figure 9: Number of false positive and false negative tree detections depending on the grouping radius. In (a), neither filtering nor the classifier are used. In (b), only filtering is used. In (c), both filtering and the classifier are used. The results indicate that filtering and the classifier are effective in avoiding false negative and false positive tree detections.